Faccio et al. Nano Convergence 20152:9
DOI 10.1186/s40580-014-0040-4

Nano Convergence
a SpringerOpen Journal

RESEARCH Open Access

Charge transfer between photosynthetic proteins and hematite in bio-hybrid photoelectrodes for solar water splitting cells

Greta Faccio[1], Krisztina Gajda-Schrantz[2,3,4], Julian Ihssen[1], Florent Boudoire[2,5], Yelin Hu[2,6], Bongjin Simon Mun[7], Debajeet K Bora[2], Linda Thöny-Meyer[1] and Artur Braun[2*]

Abstract

Functionalization of the hematite photoanode with the photosynthetic light antenna protein C-phycocyanin (PC) can yield substantial enhancement of the photocurrent density. Photoelectrochemical cells with bio-hybrid electrodes from photosynthetic proteins and inorganic semiconductors have thus potential for the use in artificial photosynthesis. We investigate here processing routes for the functionalization of hematite photoanodes with PC, including *in situ* co-polymerization of PC with enzymatically-produced melanin, and using a recombinant PC genetically engineered to carry a hexa-histidine tag (αHisPC). First, the effect of the immobilisation of PC on the electrode morphology and photocurrent production is evaluated. Then, the electronic charge transfer in dark and light conditions is assessed with electrochemical impedance spectroscopy and valence band (VB) X-ray photoemission spectroscopy. The relative shift of the VB spectrum towards the Fermi energy E_F upon illumination is smaller for the more complex processed coating and virtually disappears for αHisPC immobilised with a melanin film. Optimal conditions for protein immobilisation are determined and the dark currents benefit most from the most advanced protein coating processes.

Keywords: Artificial photosynthesis; Antenna protein C-phycocyanin; Hematite photoanode; Impedance spectroscopy; Valence band (VB) X-ray photoemission spectroscopy

1 Background

Hematite, a ferric oxide with 2.1 eV optical band gap energy, is considered a low cost and environmentally benign photoanode material for solar hydrogen production by water splitting in photoelectrochemical cells (PEC). The research and development of photoelectrodes for PEC is focused on the tailoring of the electronic structure and the microstructure, and recently also on the design of hetero structures. The functionalization of a photoelectrode with light harvesting proteins was recently demonstrated for hematite using C-phycocyanin (PC) [1], which constitutes basically a dye sensitization.

Dye sensitization [2] is an established technology for the extension of the light absorption range of inorganic photoelectrodes for solar energy conversion. To be fully functional, the electric charge generated in the dye upon light absorption needs to be transferred to the photoelectrode, i.e. the interface between the dye and the photoelectrode must warrant proper charge transfer for electrons or holes.

We recently developed a process which enhances the photocurrent of hematite thin-film electrodes by immobilising light-harvesting proteins such as PC on the surface [1]. So far, the functionalization has been performed with the commercially available PC from *Spirulina* sp. which contains the α- and β-subunits of the protein. In the present study, we evaluate the simpler α-subunit of PC from *Synechocystis* sp. PCC6803 which is recombinantly produced in *E. coli* and engineered to carry an N-terminal hexa-histidine tag (αHisPC) [3]. The electronic charge transfer is investigated by electrochemical impedance spectroscopy (EIS) and with valence band X-ray photoemission spectroscopy (VB PES).

* Correspondence: Artur.Braun@alumni.ethz.ch
[2]Laboratory for High Performance Ceramics, Empa, Swiss Federal Laboratories for Materials Science and Technology, Überlandstrasse 129, 8600 Dübendorf, Switzerland
Full list of author information is available at the end of the article

2 Methods

2.1 Materials

1,1′-Carbonyldiimidazol (CDI, >97%), 1,4-dioxane (99.8%), 2,2′-azino-bis(3-ethylbenzothiazoline-6-sulfonic acid) diammonium salt (ABTS, >98%), monopotassium phosphate (1 mol l^{-1}), hydrogen dipotassium phosphate (1 mol l^{-1}), potassium hydroxide (KOH, 95%), iron nitrate nonahydrate (>98%), tetrahydrofuran (THF, >99.9%), sodium chloride (NaCl, 5 mol l^{-1}), L-tyrosine (>99%), Tris–HCl (>99%) and C-phycocyanin isolated from *Spirulina* sp. (99.9%) were purchased from Sigma-Aldrich. Oleic acid (>60%) and L (+)-tartaric acid (>99.5%) were purchased from Fluka. Tyrosinase from *Verrucomicrobium spinosum* was produced in *E. coli* and proteolitically activated as described in [4].

2.2 Production and purification of C-phycocyanin from *Synechocystis* sp. PCC6803

The α-subunit of PC from *Synechocystis sp.* PCC6803 was produced in an N-terminally His-tagged form according to [3] and purified with a modified protocol from [5]. Briefly, strain *E. coli* DH5α was co-transformed with plasmids pAT101 and pBD414V and transformants were selected for resistance to both kanamycin (50 μg ml^{-1}) and spectinomycin (100 μg ml^{-1}). Cultures were routinely set up in TB medium (500 ml volume), incubated at 37°C under constant shaking (180 rpm), and expression was induced by adding IPTG (final conc. 1 mM). Cells were harvested by centrifugation 17 h post-induction and stored at −20°C. Upon thawing and re-suspension in 100 mM potassium phosphate buffer with pH 7.5 (5 ml g^{-1} wet cell weight), lysozyme (final conc. 1 mg ml^{-1}) and a protease inhibitor mix (Complete Protease Inhibitor Cocktail Tablets, Roche) were added. The cell suspension was then subjected to a freeze-thaw cycle at −20°C. Cells were further disrupted by sonication, and the cell-free extract, isolated by ultracentrifugation, was loaded onto a HisTrap column (1 ml, GE Healthcare Life Sciences) for purification by immobilized metal ion affinity chromatography (IMAC). αHisPC was eluted with imidazole (conc. 200 mM) in 100 mM potassium phosphate (pH 7.5). αHisPC-containing fractions were concentrated and desalted with a Vivaspin ultrafiltration device (10000 cut-off, Sartorius). The purified αHisPC was stored at −20°C for further use. Protein concentrations of αHisPC solutions were determined spectrophotometrically with a Synergy Mx spectrophotometer (Biotek, Switzerland) and using an extinction coefficient of 140000 M^{-1} cm^{-1} at 620 nm. Protein purity was assessed spectrophotometrically as the ratio of the absorbance at 280 nm and at 620 nm.

2.3 Hematite films and single crystals

Hematite films were prepared as described previously [6]. Fluorine doped tin oxide (FTO) coated glass slides (12 mm × 30 mm × 2 mm, TEC-8 from Hartford Glass Inc.) were automatically dip coated (DipMasterTM-50, Chemat Technology Inc., USA) with the precursor solution and dried at 75°C for 5 min on a hot plate. The samples were then further annealed for 30 min at 500°C in an air vented muffle furnace. Dip coating and annealing were repeated three times so as to obtain a film of four layers of hematite, which has typically a thickness of 500 to 600 nm. Prevalence of the hematite phase was confirmed with X-ray diffraction (Siemens D5000).

The thickness of the hematite films was determined with a mechanical profilometer (XP-1 Stylus Profiler by Ambios Technology). The morphology of the pristine and protein coated hematite films was investigated with a Philips XL 30 scanning electron microscope (SEM, Oxford instruments).

Hematite single crystals with (0001) orientation were purchased from SurfaceNet GmbH, Rheine, Germany. They had a size of 5 mm × 5 mm × 1 mm size and were Epi surface polished.

2.4 Coating of hematite with proteins and melanin

Similarly to [1], the hematite thin films were first dip-coated with a 0.001% agarose solution, let dry, and second with ~100 μl cm^{-2} of a 30 mg ml^{-1} CDI solution prepared in dioxan. Protein immobilisation was carried out by coating the hematite surface with a melanin-forming mixture containing PC or αHisPC (concentration 0.2 mg ml^{-1}), L-tyrosine (concentration 0.1 mg ml^{-1}), and tyrosinase (50 μg ml^{-1} concentration) in 0.05 M phosphate buffer saline (PBS; 160 g l^{-1} NaCl, 4 g l^{-1} KCl, 28.88 gl^{-1} Na_2HPO_4, 4.4 g l^{-1} KH_2PO_4, pH 7.2-7.4) for 3 h. The surface was dried between all the steps, eventually rinsed with PBS and distilled water, and then stored at 4°C in the dark until the actual measurements were performed. Because the tyrosinase preparation contains traces of trypsin, the protease inhibitor phenylmethanesulfonyl fluoride (PMSF) was added to the coating mixture at a 1 mM final concentration. The thickness of the films treated with melanin alone, or with melanin plus PC or with melanin plus αHisPC was below 1000 nm. All samples were prepared in either duplicate or triplicate and average values are reported throughout this paper.

In addition to the aforementioned thin hematite films on FTO-coated glass slides, three (0001) hematite single crystals were coated with:

1) Melanin plus αHisPC: 50 μl solution containing αHisPC, L-tyrosine and tyrosinase in PBS (concentrations as above) after pre-treatment of the hematite single crystal with agarose and CDI solution (as described above).

2) PC only: 50 μl solution containing PC, after pre-treatment of the hematite single crystal with agarose and CDI solution (as described above).

3) Melanin plus PC: 50 μl solution containing PC and the melanin-forming mixture (as described above), after

pre-treatment of the hematite single crystal with agarose and CDI solution (as described above).

2.5 Photoelectrochemical assessment of the films

For the assessment of the photoelectrochemical properties of the photoanode, we largely followed the recommendations provided in [7], when not otherwise stated in this manuscript. Linear voltammetry in the dark and under illumination was conducted using a specifically designed spectro-photoelectrochemical cell (known as EPFL cappuccino cell) made of polyether ether ketone (PEEK) and a potentiostat (Voltalab80 PGZ 402). The hematite photoanode was connected as the working electrode in a three electrode configuration. A platinum sheet of 5 mm × 5 mm was used as counter electrode and an Ag/AgCl (with saturated KCl) electrode was used as reference electrode. The electrolyte was 0.05 M PBS. Sunlight was simulated by a 1 Sun Oriel Lamp (L.O.T.–Oriel AG) with a quartz filter, corresponding to AM 1.5 global standard solar spectrum. The bias potential was scanned from 0 mV to 1000 mV. All shown results are the arithmetic average of data of at least three consecutive measurements. Electrochemical impedance spectra were recorded with the Voltalab80 PGZ 402 using the same cell in the frequency range from 100 kHz to 100 mHz with 20 data points per decade and a perturbation amplitude of 10 mV. Spectra of hematite films coated on FTO glass and of variously prepared PC films on hematite were recorded. Dark and light conditions as described above were applied during the impedance measurements.

2.6 Photoemission spectroscopy

X-ray photoemission (PES) spectra were recorded at beamline 8–1 at Stanford Synchrotron Radiation Lightsource, Menlo Park, CA. Specifically, the spectra were recorded under Fe 2p resonant condition with 53.2, 54.4 and 55.8 eV photon energy, so that the valence band spectra were particularly representing the Fe relevant features. The PES spectra were measured from the surface finished (0001) hematite single crystals that were coated with PC in the aforementioned different processing routes. The measurements of PES were carried out under ultrahigh vacuum condition, i.e. 10^{-10} mbar base pressure. At the time of experiment, the films could be considered dry by ambient conditions. A 1.5 AM solar simulator (HAL-302 Solar Simulator, 350–750 nm, Asahi Spectra, Japan) was used to illuminate the samples during the PES experiments.

3 Results and Discussion

We have recently observed that the photocurrent density of a hematite electrode increases when the light-harvesting protein phycocyanin (PC) is copolymerized with melanin on its surface. In the present work we investigate the influence of PC concentration, the time of incubation with the melanin-forming mixture on the photocurrent. In addition to the commercially available PC preparation, we test the effect of a recombinantly produced form of PC on the performance of the photoelectrochemical cell (PEC). Each sample is measured prior to and after the immobilization of proteins under pH-neutral conditions in PBS, if not mentioned otherwise.

3.1 Production of recombinant αHisPC

The α-subunit of PC from *Synechocystis sp.* PCC6803 is produced in recombinant form in *E. coli* with a two-plasmid system [3]. Carrying an N-terminal Hexahistidine tag, αHisPC is purified by immobilized metal ion affinity chromatography (IMAC). The solution containing the purified αHisPC has a vivid blue colour. Differently from PC that has a maximum absorbance peak at 620 nm, the purified αHisPC shows maximum optical absorbance at 626 nm (Figure 1).

Glazer et al. reported that the peak of maximum absorbance of C-phycocyanin when composed of both α- and β-subunits results from the sum of the absorbance peaks of both subunits. The α-subunit absorbs at a longer wavelength than the β-subunit, e.g. the α-subunit has an absorbance maximum at 620 nm and the β-subunit at 608 nm in C-phycocyanin from *Synechococcus* sp. [9].

Similarly to what has been reported for PC [8], incubation under alkaline conditions, e.g. in the presence of 1 M KOH, absorbance in the 600–620 nm region is rapidly annulled and a novel absorbance peak at 750 nm is detected (Figure 1).

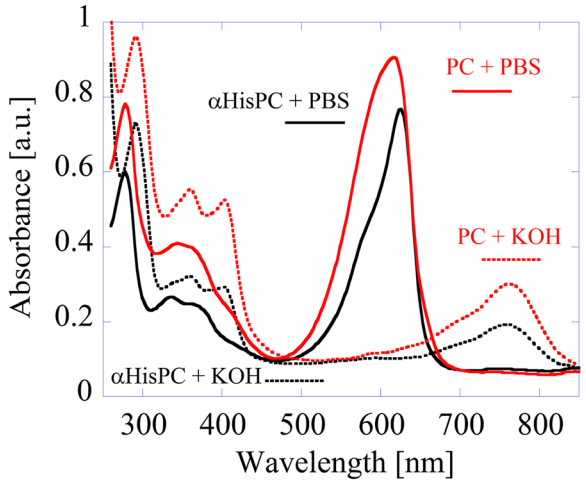

Figure 1 UV–vis spectra of PC (conc. 0.2 mg ml^{-1}, red line) and αHisPC (conc.0.2 mg ml^{-1}, black line) in the native form in PBS pH 7.4 (continuous lines) and in denatured form in 1 M KOH (dashed lines). Data for PC are reproduced from [8].

3.2 Effect of protein-melanin coating on the photocurrent

In order to establish optimal parameters for the coating process, three protein concentrations spanning two orders of magnitude (0.02, 0.2 and 2 mg ml^{-1}) and three reaction times (1.5, 3 and 4.5 h) are tested. The highest enhancement in photocurrent density was achieved at concentrations between 0.2 mg ml^{-1} to 2 mg ml^{-1} of PC and a reaction time of 3 h to 4.5 h. For hematite thin films coated with PC, the highest relative enhancement in photocurrent density is 23% and is obtained at a concentration of 2 mg ml^{-1} and a reaction time of 3 h, when measured in KOH. Under identical conditions, a higher value is obtained with samples coated with αHisPC at a concentration of 0.2 mg ml^{-1} that give a 55% increase in photocurrent density.

Figure 2 shows a typical I-V (photocurrent density) curve of the pristine and the protein coated electrodes in KOH (Figure 2a) and PBS (Figure 2b) electrolytes. The protein layer causes the higher photocurrent density. The higher photocurrent densities can be attributed to the panchromatic light harvesting action of protein and the electronic transfer to the hematite surface. The photocurrent onset potential for both samples is virtually the same vs. Ag/AgCl., i.e. ~0 V in KOH and 600 mV in PBS, when we account for the effect of the different pH on the Nernst potential.

We expect that the extreme pH conditions with the use of 1 M KOH electrolyte (~ pH 13–14) leads to melanin dissolution and structural changes in PC causing denaturation. Yet we measure in KOH a significant increase in photocurrent density (left panel, Figure 2a). A possible explanation might be found in the newly occurring absorbance feature at 750 nm for PC and αHisPC, when measured in the strongly alkaline environment (Figure 1). While the proteins may become denatured, the chromophores may still be intact and absorb light [10] and produce electron–hole pairs which add to the photocurrent. Moreover, the recombinant monomeric αHisPC appears to be a valid alternative to the commercial PC preparation. The 55% increase measured for αHisPC is significantly higher than the 8% increase measured for analogous samples prepared with PC (all measured in 1 M KOH). We thus speculate that PC and αHisPC couple differently with the surface, thus conferring different charge transfer. As a possible explanation, the presence of the Histag on αHisPC might provide a better conducting bonding to the hematite surface as histidine residues are known to coordinate iron ions and the Histag has been shown to bind iron in some proteins [11]. For the evaluation of the effect of melanin alone, samples lacking any photosynthetic protein were prepared and analysed as a control experiment. Compared to the hematite films with coatings containing PC or αHisPC and melanin, no significant increase in photocurrent was observed. Therefore the key factor for the increase in photocurrent is the biliprotein, and not the melanin. Based on these results, a 0.2 mg ml^{-1} protein concentration and 3 h enzymatic reaction time was used for further experiments.

3.3 Surface morphology of phycocyanin-melanin coated samples

Electron microscopy was used for the closer visual inspection of the hematite coated with melanin and different amounts of PC. Electron micrographs of hematite coated with melanin and PC show the formation of strands of protein-melanin complexes (Figure 3). Since the same concentration of melanin was present in all samples, strand formation depends on the protein concentration. At the lower 0.2 mg ml^{-1} protein concentration, SEM micrographs of samples coated with PC (Figure 3) shows formation of stretched dense formations in tight contact with the hematite surface, and this could play a role in the enhancement of the photocurrent. A significant strand formation is visible in samples with a PC concentration of 2 mg ml^{-1} rather than at

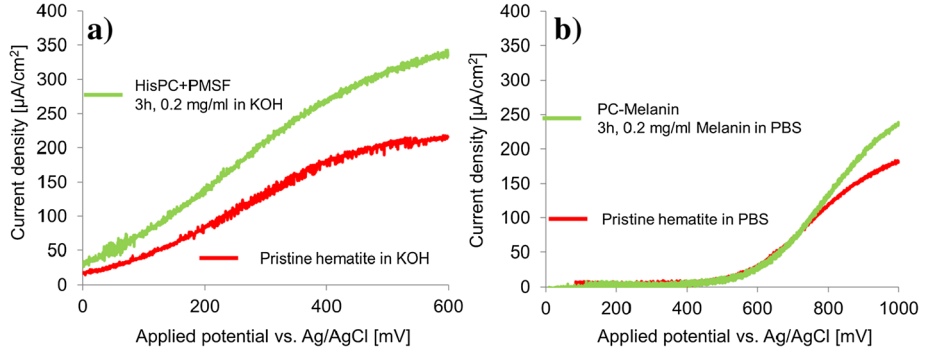

Figure 2 Photocurrent density before and after immobilization of αHisPC (a) and PC (b). Pristine hematite before (red bottom line) and after immobilization with melanin (green top line) of 0.2 mg ml^{-1} PC or αHisPC in the presence of 1 mM PMSF, for 3 h and measured in 1 M KOH (left panel) and in 0.05 M PBS (right panel).

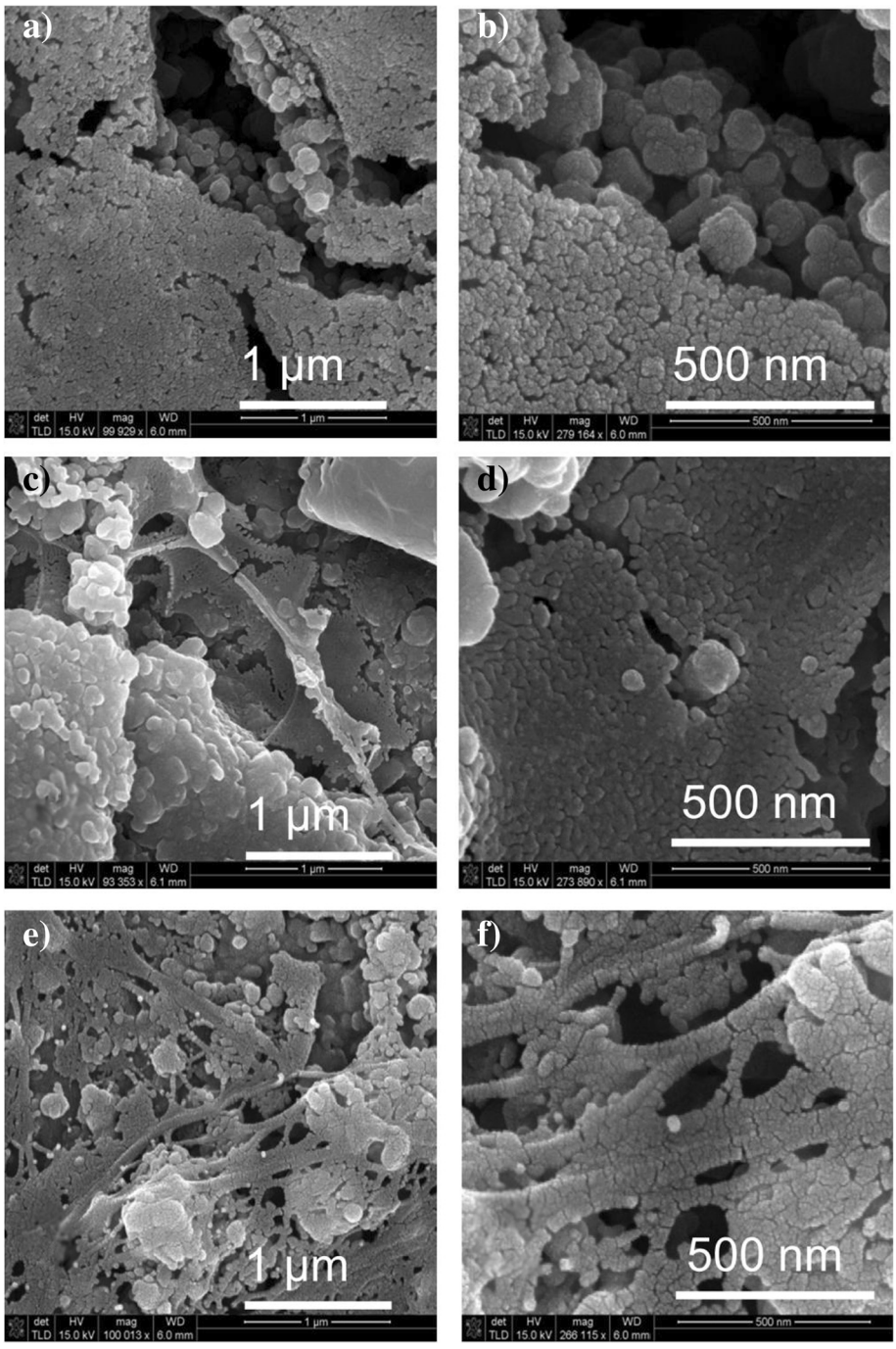

Figure 3 Scanning electron micrographs of hematite films coated with different amounts of PC, e.g. incubation for 3 h with a melanin-forming mixture containing 0.02 (a, b), 0.2 (c, d) and 2 (e, f) mg ml^{-1} incubated from top to bottom row. The scale bar is 1 μm (left) or 0.5 μm (right).

0.2 mg ml^{-1}. In addition to the protein strains, spherical granules with a diameter of 200 nm are observed (Figure 3). These are likely due to melanin which tends to organise in such granules when isolated from natural sources [12]. The pattern observed differs from that reported by Costa et al. [13] who studied natural and synthetic melanin and their interaction with Fe (III) by SEM. However, such heterogeneous kind of geometry was also described in [14] using laser light scattering which also showed how enzymatically-produced melanin can be largely hydrated and can have non-uniform density. However, the highest enhancement in current density

was measured for samples with the 0.2 mg/ml PC concentration.

3.4 Charge transfer in PC-melanin coated hematite films

Important for the functionality of bio-inorganic interfaces in sensors or energy converters is not only their physical immobilization but also sufficient charge transfer between the organic component and the inorganic component, i.e. the electrode of the current collector. Charge transfer between electrodes and proteins or even whole cells has been studied for various conducting substrates, for example for GaAs and photosystem I [15], gold and blue copper protein azurin [16], carbon nanotubes [17] and for stainless steel [18]. It is clear from numerous examples, that electrons can be directly transferred from and to proteins which are in contact with inorganic surfaces, including hematite. Impedance spectroscopy can be a valuable analytical tool for the assessment of bio-organic interfaces [19]. Dheilly et al. [20] used electrochemical impedance spectroscopy (EIS) to probe the dynamics of the charge transfer of bacterial biofilms attached to electrodes in an aqueous environment. We apply EIS for studying the interaction between the photosensitizing protein (PC) and hematite using different coating procedures under dark and illuminated conditions using PBS as electrolyte. For the reader we illustrate in Figure 4 the sequence of the various synthesis and coating steps for the assembly of the electrode.

The schematic bio-hybrid electrode architecture in Figure 5a) shows one possible impedance model circuit for our protein-semiconductor assembly (following a suggestion of Ben-Yoav et al. [22]), along with an energy diagram for the solid state processes and the processes in the electrolyte. The water splitting reaction is based on electron holes h^+ which come from the hematite photoanode: $2\ H_2O + 4\ h^+ \rightarrow O_2 \uparrow + 4H^+$. The excited PC molecule generates also an electron–hole pair. The electron moves from the PC to the hematite. Since the highest occupied molecule orbital (HOMO) energy level of PC is above the VB of hematite, the electron hole cannot transfer from PC to hematite. Rather, the hole h^+ from the PC can form with the aqueous electrolyte hydroxyl radicals ($^{\bullet}HO$) upon excitation with visible light >470 nm wavelength [23]. This would balance the charge transfer via the Type I mechanism [24]. This constitutes an electron acceptor. Backflow of electrons to the electrolyte via the surface would be prevented by the $^{\bullet}HO$ radicals. Since the electron does not get freedom to recombine with holes at the hematite surface and back injected to electrolyte, the functionalization with PC increases the photocurrent density.

Figure 6 shows the impedance spectra of the pristine hematite film coated on FTO glass, measured in PBS in the dark (Figure 6a) and under 1.5 AM solar simulated light (Figure 6b). The spectra were recorded with bias ranging from 0 mV to 1000 mV in steps of 200 mV at

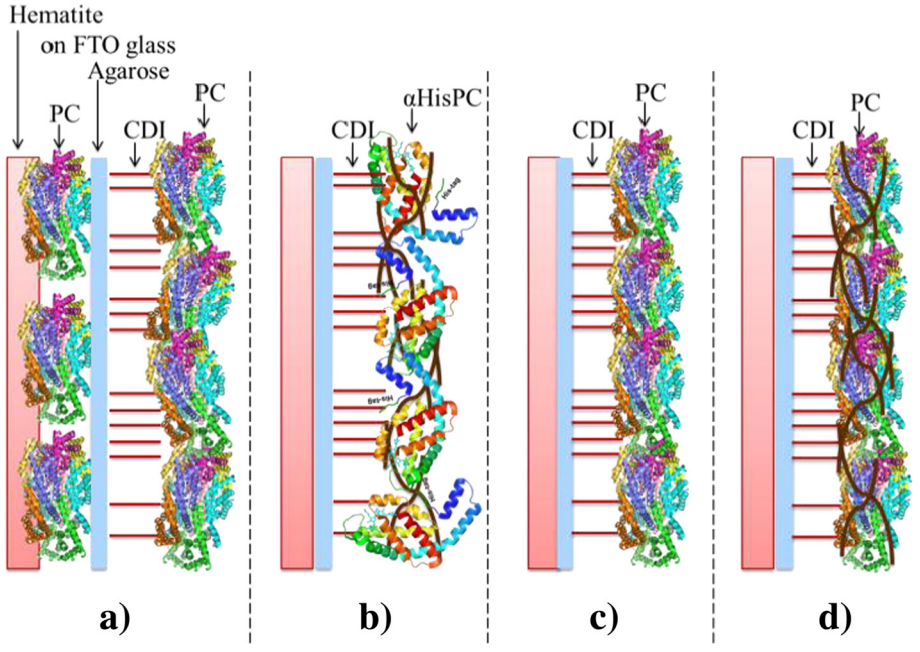

Figure 4 Schematic of the applied coating procedures for PC and αHisPC covalently attached to hematite via a chemical crosslinker, e.g. CDI. Differently from Bora [21], as shown here for reference in a), the hematite surface is directly coated with agarose and melanin using the chemical crosslinker CDI. Distances are not in proportion. Additionally, a layer containing melanin and αHisPC (**b**, upper panel, PDB ID: 4F0T), PC (**c** upper panel), or PC plus melanin (**d** upper panel, PDB ID: 1HA7) was applied.

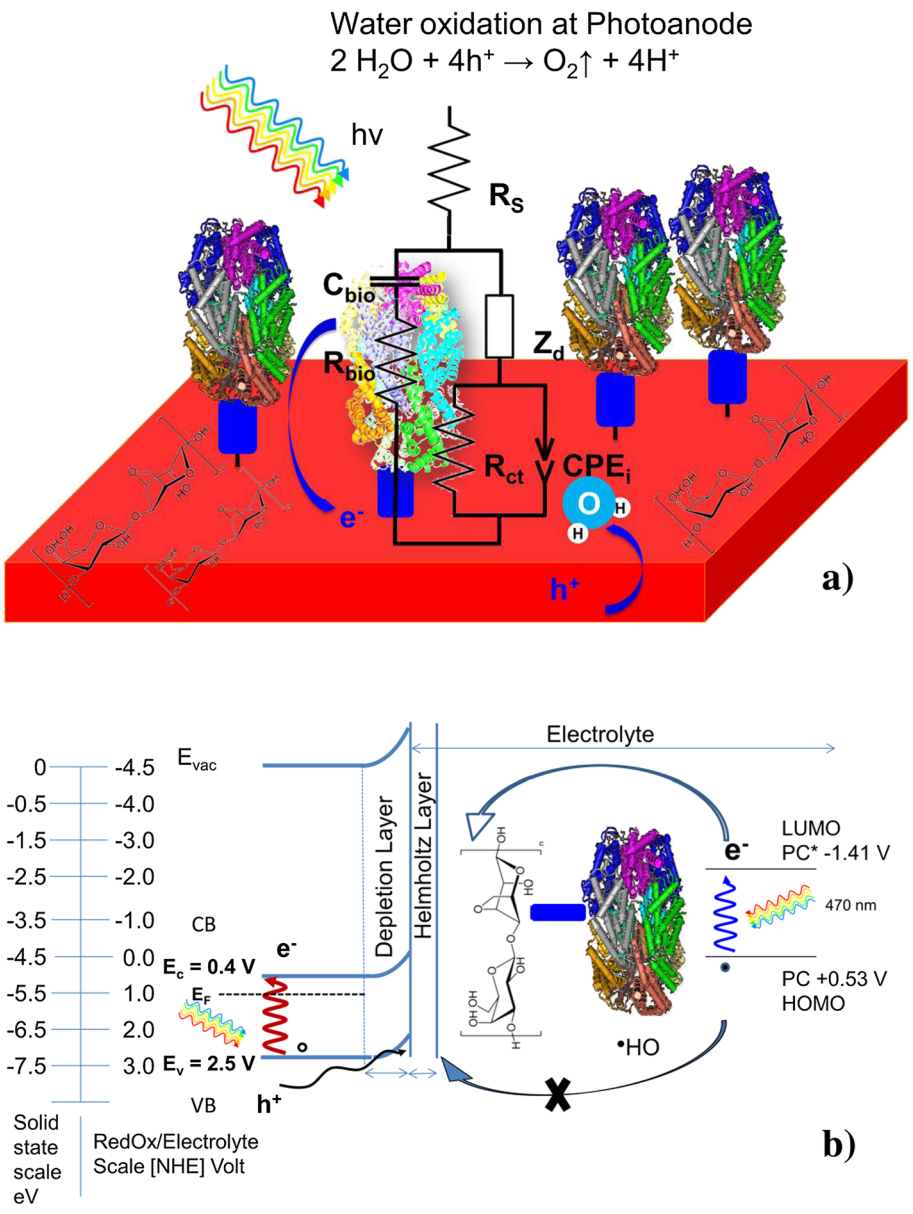

Figure 5 Top **a)** - **The semiconducting hematite interfacing the electrolyte is represented by the charge transfer resistance R_{ct} and a constant phase element CPE_i and a Warburg impedance element Z_d. R_s is the resistance of the electrolyte.** Inspired by reference [22]. Bottom **b)** – Energy diagram for the PC in aqueous electrolyte, linked with CDI and agarose to hematite.

frequencies ranging from 100 kHz (low impedance point near origin) to 0.1 Hz (high impedance point at end of spectrum). The impedance spectra of pristine hematite in dark fit in the impedance window posed by axes with 10 kOhm. Under illumination, the spectra obtained under 600 mV to 1000 mV bias show a convolution of two semicircles (Figure 6b) for the spectrum obtained at 800 mV. The first semicircle has a significantly smaller radius than the second one. The radius of the larger of both semicircles scales systematically with the applied DC bias and thus represents the charge transfer resistance.

For the hematite film coated with protein, the impedance measured in dark condition is below 5 kOhm (Figure 7a), revealing that the protein layer (αHisPC coated with the enzymatic melanin formation procedure) improves charge transfer between electrolyte and hematite. Note that we have plotted the data in Figures 6 and 7 in the same scaled window for easier comparison.

Moreover, upon illumination of the protein film, the impedance decreases dramatically (see the very small box in the lower left corner in the impedance spectrum in 7b) to far below 1 kOhm. Here it is sufficient to plot the impedance in an isometric window of 300 Ohm to

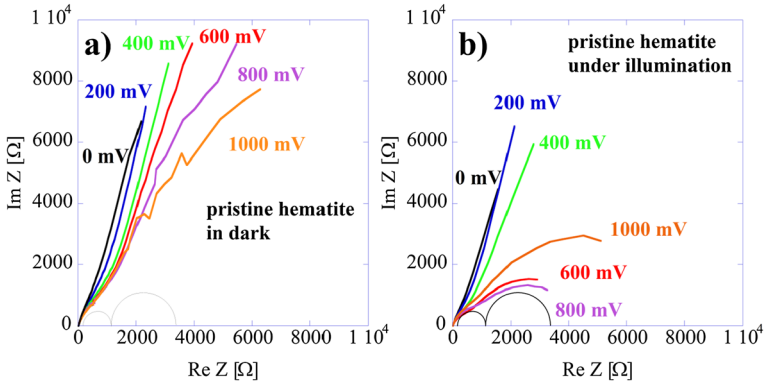

Figure 6 EIS spectra (Nyquist plots) of pristine hematite in dark a) and under illumination b) for DC bias from 0 mV to 1000 mV. The spectra are plotted on the same isometric scale.

present virtually the entire impedance spectra when measured under light condition. The lowest impedance is found for 800 mV bias. The curvature of the spectra in the inset of Figure 7b) shows the clear tendency towards semicircles as the direct current (DC) bias approaches the water splitting potential. We interpret this as increased charge transfer of the system during illumination and increased DC bias. The protein coating improves the conductivity and charge transfer between the hematite and the electrolyte also under illumination significantly. The impedance for pristine and protein coated hematite increases again in the transition from 800 mV to 1000 mV. This is, where typically considerable oxygen evolution by water oxidation takes place.

Charge transfer across interfaces depends on the electronic structure of these interfaces. A method for the assessment of the electronic structure of surfaces and interfaces is X-ray and photoelectron spectroscopy (XPS) and photoemission spectroscopy (PES). In Brizzolara et al. [25] the conclusion about covalent attachment of the proton pump protein bacteriorhodopsin via genetic substitution of cysteine for serine (S35C) was based partially on the XPS core level spectra of sulfur, i.e. via detection of the chemical shift of the sulphur core level spectrum. An early valence band (VB) XPS study on a protein (D-luciferin) is presented in Wada et al. [26], where XPS helped sketch a model for the luminescence. In this study, we find that the position of the VB spectrum changes depending on the type of phycocyanin coating process applied to hematite.

Figure 8 shows a set of VB spectra which were recorded with photoemission spectroscopy (PES) with photon energies close to the Fe 3p resonance edge, ~54 eV. The PES was employed in resonance so as to identify the contribution of the Fe ions in the VB density of states (DOS). The spectra were recorded from three different samples, Figure 8a) PC coated on hematite single crystal, Figure 8b) PC and melanin (PC + Mel) co-polymerized on hematite single crystal, and Figure 8c) His-tagged PC and melanin (αHisPC + Mel) on hematite single crystal.

We observe that, under dark condition (8a), the intensity maximum of the spectrum from the PC film shifts

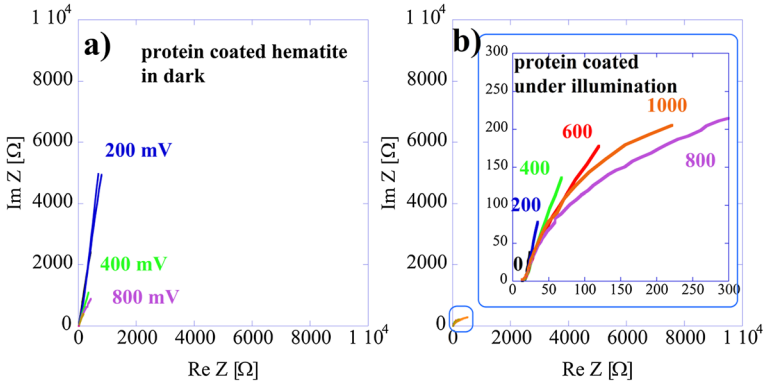

Figure 7 EIS spectra (Nyquist plots) of protein coated hematite recorded in dark a) and under illumination b) for DC bias from 0 mV to 1000 mV. The inset on the right shows the largest magnification. Note the very small window in the lower left corner, showing the very small overall impedance of the illuminated protein film. Coating procedure: enzymatic, αHisPC plus melanin (condition B in Figure 4, upper panel) [8].

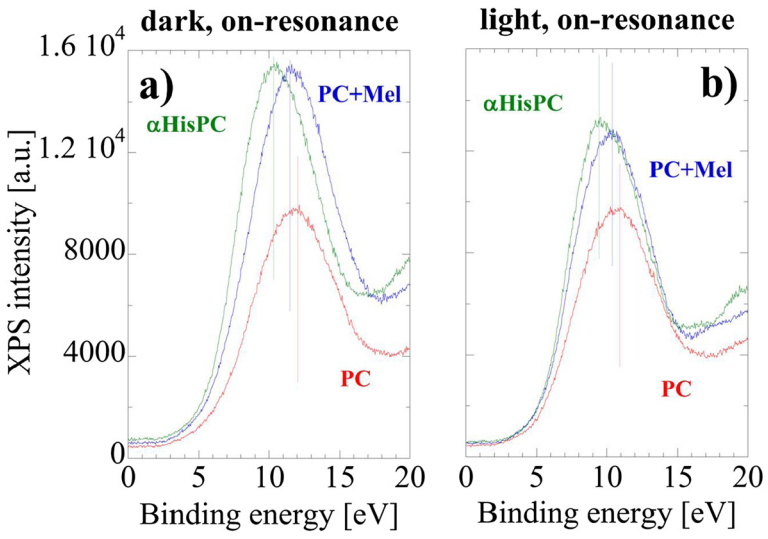

Figure 8 Comparison of three different coatings (condition B-D in Figure 4, upper panel) on hematite in Fe3p on-resonance condition at 54.4 eV photon energy under dark (a) and illuminated (b) conditions. With more advanced film processing technology, the VB PES spectra shifts closer towards the Fermi level (0 eV binding energy).

from 12 eV to just below 11.5 eV towards the Fermi level, when PC was co-polymerized with melanin (Figure 8a). With αHisPC + Mel on hematite, the intensity maximum shifts to 10.3 eV. A similar trend is shown in the case of illumination with the solar simulator (Figure 8b). We notice that with increasing improvement of film processing technology, the maxima of the VB spectra move closer to the Fermi level E_F, reflecting the changes in the electronic structure with increased DOS near E_F. The charge transfer between hematite and phycocyanin might be improved in αHisPC as histidines are known to coordinate to iron ions. At this time it is not clear whether the spectral shift towards the E_F is a result of hole doping originating from the PC + Mel in the films. In addition, the His-tag presumably improves entrapment of the His-tagged protein into the melanin network, as the formation of histidine-tyrosine bonds have been observed upon tyrosinase-catalysed crosslinking [27].

It is clear, however, that there is a correlation between improved electric transport, increased photocurrent and increased DOS in the VB near E_F. Although literature on the electronic structure of the interfaces of biological macromolecules and inorganic materials is scarce, some pioneering studies have been published. A PES and NEXAFS study on the electronic structure of an ultra-thin film of the surface layer of *Bacillus sphaericus* deposited on Si wafers showed how the highest occupied and lowest unoccupied molecular orbitals (HOMO and LUMO) constitute the band gap of the assembly [28]. In an extension of that study, these authors showed with resonant PES how charge transport evolved from torsion effects in the protein [29].

We want to turn to another observation in our PES spectra. When subjecting the protein-hematite assembly to 1.5 AM simulated solar light, the spectral weight of the intensity range near the O2p bonding peak decreases and shifts by up to 0.7 eV toward the Fermi level (0 eV binding energy).

We interpret this shift as the hole-doped DOS resultant from the exposure of visible light. With the solar lighting on, the electron–hole pairs can be created in the conduction band (CB) and the holes stays near the surface generating a p-type DOS. A similar trend of binding energy shift is observed when silicon is doped [30]. Our PES studies on proteins are in principal not different from studies on synthetic organic molecules and polymers which are frequently used in solar cells and light emitting diodes. A comprehensive review on such VB spectroscopy studies is presented by Koch et al. [31].

Among our protein functionalization processes, the coating with PC only (Figure 9a) is the least complex one. For the comparison of the PES spectra in Figure 9, we determine the position of the VB by extrapolation of the spectral flank near E_F towards zero intensity – as a simple and practical metric. The intercept is then by our definition the VB position. The VB position of the PES spectra shifts from 6 eV to 5 eV when the sample is illuminated with the solar simulator (Figure 9a). This 1 eV shift thus originates from the illumination effect, i.e. a charge carrier (electron hole pair) generation.

When we turn to the PC + Mel coated hematite (Figure 9b), the VB position shifts from 5.6 eV to 5 eV, i.e. the shift is only 0.6 eV upon illumination. In the case of the HisPC coating (Figure 9c), there is no shift of the VB spectrum

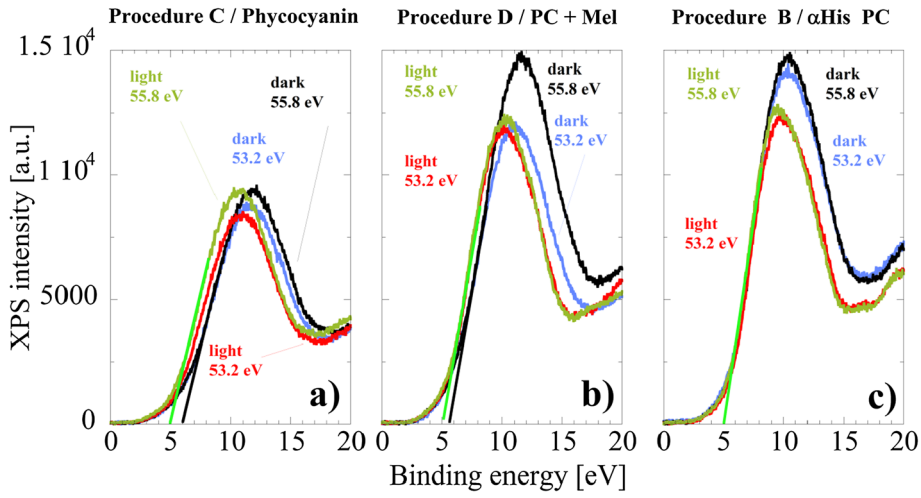

Figure 9 Comparison of VB PES spectra for the three different protein coatings (procedures C, D, and B from left to right from Figure 4). The steep straight lines intersecting near 5 eV show the VB position. The sample coated with PC and melanin (panel **b**), procedure D in Figure 4) shows 0.6 eV shift on VB position while PC only (panel **a**), procedure C in Figure 4) shows 1.0 eV shift under illumination. In the case of αHisPC (panel **c**)), no shift in the VB position is observed.

when the light is switched on. Interestingly, for all films, the position of the VB in the illumination condition is 5 eV. Hence, it appears that light has no influence on the charge transfer as far as the interface of the protein film with the hematite is concerned.

In addition to the electric charge transfer, which is the scope of this paper, fluorescence resonance energy transfer (FRET) could hypothetically occur between phycocyanin and hematite and thus increase the photocurrent density. The efficiency of the FRET mechanism is inversely proportional to the sixth power of the distance between light donor and light acceptor, making it extremely sensitive to distances and virtually negligible for small distances. Due to the architectures of our bio-hybrid electrodes, where agarose, CDI and His tag virtually constitute “spacers” between PC and hematite, it is difficult to perceive that FRET could occur across these spacers.

4 Conclusions

The immobilization of photosynthetic proteins on hematite, in particular C-phycocyanin, yields a substantial increase of the photocurrent density which can be assigned to electron hole pair formation in the protein by light absorption in a wavelength range that exceeds the absorption range of the hematite. Refined immobilization strategies like co-polymerization of PC with melanin or genetic engineering to attach a His-Tag to PC successively increase the photocurrent. Analysis of the charge carrier dynamics of the bio-hybrid electrode assembly under photoelectrochemical conditions shows that upon illumination the enhanced charge transfer and DC bias are substantially amplified (factor 10) when the hematite film is coated with the light harvesting protein. This, however, seems to have not the same strong effect on the photocurrent density (only factor 2). A clear and systematic dependency of spectral shift of the valence band is observed in the dark and in the illuminated condition. While the His-tag strategy clearly improves the charge transfer between PC and hematite in the dark, no further enhancement is observed under illumination condition. This might be due to the fact that the illumination generates electron hole pairs, but this should have no effect on the charge transport characteristic of the covalent linkages between protein and hematite.

Competing interests

The authors declare that they have no competing interests.

Authors’ contributions

GF synthesized and processed samples and wrote major part of the manuscript. KGS synthesized and processed samples and measured current densities. JI organized the work, inspired the use of melanin and provided intellectual input on protein functionalization. FB measured the protein samples with photoemission spectroscopy at SSRL and ALS. YH measured the protein samples with photoemission spectroscopy at SSRL and ALS and analyzed the impedance spectra and arranged for SSRL beamtime. BSM measured the protein samples with photoemission spectroscopy at SSRL and ALS and discussed the spectra. DKB provided intellectual input in. LTM organized the work and provided intellectual input. AB organized the work, inspired the protein functionalization, provided intellectual input, did data analysis on photoemission spectra, arranged for ALS beamtime and wrote major part of the manuscript. All authors read and approved the final manuscript.

Acknowledgements

This study was funded at large by the VELUX Foundation under project no° 790 (Biomimetic photoelectrochemical cells for solar hydrogen generation: Bio-PEC) for K. G.-S. and G.F. G.F. was also financially supported by the TYROMAT project (COFUND action between Empa Postdocs programme and FP7: People) and COST TD1102 Action Project by SBFI C13.003. Financial support by the Strategic Korean-Swiss Cooperative Program in Science and

Technology within the project "Spectroscopy on photoelectrochemical electrode materials: SOPEM" for A.B. and NRF-2013K1A3A1A14055158 for B.S.M. is gratefully acknowledged. Financial support by the Swiss National Science Foundation for F.B. (project # 200021–137868 Reaction–diffusion processes for the growth of patterned structures and architectures: bottom up approach for photoelectrochemical electrodes) and for Y.H. (project # 200021–132126 Defects in the bulk and on surfaces and interfaces of metal oxides with photoelectrochemical properties: In-situ photo-electro-chemical and resonant x-ray and electron spectroscopy studies) and R'Equip # 121306 is gratefully acknowledged.
Portions of this research were carried out at the Stanford Synchrotron Radiation Lightsource, a national user facility operated by Stanford University on behalf of the U.S. Department of Energy, Office of Basic Energy Sciences. The solar simulator was provided by Jinghua Guo, Advanced Light Source in Berkeley. Florian Häussler (Empa Dübendorf) assisted with the sample preparation at Empa. We are grateful to Prof. Wendy Schluchter from the Department of Biological Sciences of the University of New Orleans for providing the plasmids for the production of αHisPC in this study.

Author details
[1]Laboratory for Bioactive Materials, Empa, Swiss Federal Laboratories for Materials Science and Technology, Lerchenfeldstrasse 5, 9014 St. Gallen, Switzerland. [2]Laboratory for High Performance Ceramics, Empa, Swiss Federal Laboratories for Materials Science and Technology, Überlandstrasse 129, 8600 Dübendorf, Switzerland. [3]Department of Inorganic and Analytical Chemistry, Szeged University, Dóm tér 7, H-6720 Szeged, Hungary. [4]Institute of Chemistry, Research Group of Environmental Chemistry, University of Szeged, Rerrich Béla tér 1, H-6720 Szeged, Hungary. [5]Department of Chemistry, University of Basel, Spitalstrasse 51, 4056 Basel, Switzerland. [6]Laboratory for Photonics and Interfaces, Ecole Polytechnique Federale de Lausanne, Rue Cantonale, 1021 Lausanne, Switzerland. [7]Department of Physics and Photon Science, GIST School of Physics and Chemistry, GIST College, Ertl Center for Electrochemistry and Catalysis, 123 Cheomdan-gwagiro (Oryong-dong), Buk-gu, Gwangju 500-712, Korea.

Received: 2 November 2014 Accepted: 7 November 2014
Published online: 06 May 2015

References

1. Bora DK, Braun A, Constable EC: Energy Environ. Sci. 2013, **6**(2):407–425.
2. Anderson S, Constable EC, Dare Edwards MP, Goodenough JB, Hamnett A, Seddon KR, Wright RD: *Nature* 1979, **280**(5723):571–573.
3. Tooley AJ, Cai YP, Glazer AN: Proc. Natl. Acad. Sci. 2001, **98**(19):10560–10565.
4. Fairhead M, Thoeny-Meyer L: *New Biotechnol* 2012, **29**(2):183–191.
5. Taurino I, Reiss R, Richter M, Fairhead M, Thoeny-Meyer L, De Micheli G, Carrara S: Electrochim. Acta. 2013, **93:**72–79.
6. Hu Y, Bora DK, Boudoire F, Haeussler F, Graetzel M, Constable EC, Braun A: J. Renew. Sust. Ener. 2013, **5**(4):043109.
7. Chen Z, Jaramillo TF, Deutsch TG, Kleiman-Shwarsctein A, Forman AJ, Gaillard N, Garland R, Takanabe K, Heske C, Sunkara M, McFarland EW, Domen K, Miller EL, Turner JA, Dinh HN: J. Mater. Res. 2010, **25**(1):3–16.
8. Ihssen J, Braun A, Faccio G, Gajda-Schrantz K, Thöny-Meyer L: **Light harvesting proteins for solar fuel generation in bioengineered photoelectrochemical cells.** Curr. Protein. Pept. Sci. 2014, **15: in press.**
9. Glazer AN, Fang S, Brown DM: J. Biol. Chem. 1973, **248:**5679–5685.
10. Berns DS, MacColl R: Chem. Rev. 1989, **89:**807–825.
11. The Recombinant Protein Handbook: **Protein amplification and simple purification.** *Amersham Biosciences* 2002, 41–58. 18-1142-75.
12. Watt AA, Bothma JP, Meredith P: *Soft Matter* 2009, **5**(19):3754–3760.
13. Costa TG, Younger R, Poe C, Farmer PJ, Szpoganicz B: Bioinorg. Chem. Appl. 2012, **2012:**712840.
14. Bridelli MG: Biophys. Chem. 1998, **73**(3):227–239.
15. Frolov L, Rosenwaks Y, Richter S, Carmeli C, Carmeli I, Phys J: Chem. C. 2008, **112:**13426–13430.
16. Chi Q, Farver O, Ulstrup J: *PNAS* 2005, **102**(45):16203–16208.
17. Deng S, Jian G, Lei J, Hu Z, Ju H: *Biosens Bioelectron* 2009, **25:**373–377.
18. Omanovic S, Roscoe SG: Langmuir 1999, **15**(23):8315–8321.
19. Owino IOK, Sadik OA: *Electroanalysis* 2005, **17**(23):2101–2113.
20. Dheilly A, Linossier I, Darchen A, Hadjiev D, Corbel C, Alonso V: Appl. Microbiol. Biotechnol. 2008, **79**(1):157–164.
21. Bora DK, Rozhkova AA, Schrantz K, Wyss PP, Braun A, Graule T, Constable EC: Adv. Funct. Mater. 2012, **22**(3):490–502.
22. Ben-Yoav H, Freeman A, Sternheim M, Shacham-Diamand Y: Electrochim. Acta. 2011, **56**(23):7780–7786.
23. Zhang S, Xie J, Zhang J, Zhao J, Jiang L: Biochim. Biophys. Acta. 1999, **1426**(1):205–211.
24. Foote CS: Photochem. Photobiol. 1991, **54**(5):659.
25. Brizzolara RA, Boyd JL, Tate AE, Vac J: Sci. Technol. A. 1997, **15**(3):773–778.
26. Wada N, Shitaba R, Shibazaki M, Suzuki N: Photochem. Photobiol. 1989, **49**(4):513–518.
27. Hellman M, Mattinen M-L, Fu B, Buchert J, Permi P: J. Biotechnol. 2011, **151**(1):143–150.
28. Vyalikh DV, Danzenbacher S, Mertig M, Kirchner A, Pompe W, Dedkov YS: Phys. Rev. Lett. 2004, **93**(23):238103.
29. Vyalikh DV, Maslyuk VV, Blueher A, Kade A, Kummer K, Dedkov YS: Phys. Rev. Lett. 2009, **102**(9):098101.
30. Sezen H, Suzer S: J. Chem. Phys. 2011, **135:**141102.
31. Koch N: phys. stat. sol. RRL. 2012, **6**(7):277–293.